A comparison of six DNA extraction protocols for 16S, ITS, and shotgun metagenomic sequencing of microbial communities

Justin P. Shaffer[1], Carolina S. Carpenter[2,3], Cameron Martino[1,3,4], Rodolfo A. Salido[1,5], Jeremiah J. Minich[6], MacKenzie Bryant[1], Karenina Sanders[1], Tara Schwartz[1], Gregory Humphrey[1], Austin D. Swafford[3,7], Rob Knight[1,3,8,9,*]

1. *Department of Pediatrics, University of California, San Diego, La Jolla, CA*
2. *Scripps Institution of Oceanography, University of California, San Diego, La Jolla, CA*
3. *Center for Microbiome Innovation, University of California, San Diego, La Jolla, CA*
4. *Bioinformatics and Systems Biology Program, University of California San Diego, La Jolla, CA*
5. *Department of Bioengineering, University of California San Diego, La Jolla, CA, USA.*
6. *Marine Biology Research Division, University of California, San Diego, La Jolla, CA*
7. *InterOme, Inc. Carlsbad, CA*
8. *Micronoma Inc. San Diego, CA*
9. *Department of Computer Science and Engineering, University of California, San Diego, La Jolla, CA*

* *Corresponding author*

Abstract.
Microbial communities contain a broad phylogenetic diversity of organisms, however the majority of methods center on describing bacteria and archaea. Fungi are important symbionts in many ecosystems, and are potentially important members of the human microbiome, beyond those that can cause disease. To expand our analysis of microbial communities to include fungal ITS data, we compared five candidate DNA extraction kits against our standardized protocol for describing bacteria and archaea using 16S rRNA gene amplicon and shotgun metagenomics sequencing. We present results considering a diverse panel of host-associated and environmental sample types, and comparing the cost, processing time, well-to-well contamination, DNA yield, limit of detection, and microbial community composition among protocols.

Accession numbers. Raw sequence data were deposited at the European Nucleotide Archive (accession#: ERP124610) and raw and processed data are available at Qiita (Study ID: 12201). All processing and analysis code is available on GitHub (github.com/justinshaffer/Extraction_kit_testing).

Methods summary.
To allow for downstream applications involving fungi in addition to bacteria and archaea, we compared five DNA extraction kits with our previously established, standardized protocol for extracting DNA for microbial community analysis. Across ten diverse sample types, we found one extraction kit to perform comparably or better than our standardized protocol. Our conclusion is based on per-sample comparisons of DNA yield, the number of quality-filtered

sequences generated, the limit of detection of microbial cells, microbial community alpha-diversity, beta-diversity, and taxonomic composition, and extent of well-to-well contamination.

Keywords: amplicon, internal transcribed spacer, Katharoseq, limit of detection, MagMAX Microbiome, MagAttract PowerSoil, mock community, rRNA, well-to-well contamination, whole genome sequencing

Introduction.

Research into microbial communities continues to reveal links that help to support both human and environmental sustainability [1-4]. In order to properly identify important connections between microbiota and human health and well-being [5-7], parallel work must foster the innovation of methods that refine our view of microbial communities [4, 8-10]. However, widespread adoption of standardized methods for performing microbiome studies continues to be hindered by a lack of approaches that capture information from all organisms, or from across diverse sample types [11-13].

Whereas methods for capturing information from bacteria and archaea have been well-developed and widely adopted, those that additionally consider microbial eukaryotes such as fungi have received less attention [14-16]. Similar to bacteria and viruses for mammals, fungi are the most important plant pathogens worldwide [17,18] and represent an increasing threat to certain groups of animals, including amphibians [19-21]. Fungi are also invaluable components of soils and forests [22-24], and are currently emerging as important members of the human microbiome (*i.e.*, mycobiome) [25-27]. Currently, our protocol for DNA extraction for high-throughput microbiome sequencing focuses on describing bacterial/archaeal taxa, and has not yet been tested to additionally describe Fungi.

Here, we aimed to identify an extraction kit that extracts DNA from fungal communities while also producing DNA output and community composition for bacteria/archaea similar to our previously established, standardized protocol [28]. We compared DNA yield, the number of quality sequences, microbial community alpha- and beta-diversity and taxonomic composition, and also technical differences in the limits of detection of bacterial and fungal cells [29], and the extent of sample-to-sample (*i.e.*, well-to-well) contamination [30-32] among extraction protocols.

Materials & Methods.

Sample collection. To compare each candidate extraction kit against our standardized protocol, we collected a wide selection of human- and environmental samples, focusing on types widely used in studies of microbial communities [28,33]. Each unique sample was aliquoted across extraction plates of all kits for comparison of extraction efficiency. We included a total of 6 human skin samples, 6 human oral samples, 4 built environment samples, 10 fecal samples, 6 human urine samples, 2 human breastmilk samples, 6 soil samples, 4 water samples, 4 fermented food samples, and 2 tissue samples. Except where described otherwise below, we collected samples using Puritan wood-handled, cotton swabs, following the Earth Microbiome Project standard protocol [14].

We collected samples in a way that allowed technical replication across extraction protocols (*i.e.*, three technical replicates per protocol). Human skin samples included those from the foot and armpit, which were collected from three individuals by rubbing five cotton swabs simultaneously on the sole of each foot or armpit, respectively, for 30 s. Human oral samples included saliva, which was collected from 12 individuals by active spitting into a 50 mL centrifuge tube. Built environment samples included floor tiles and computer keyboards. Floor and keyboard samples were collected from two laboratory bays or two computers, respectively, using cotton swabs, by rubbing nine swabs simultaneously across the surface of a 0.3 m^2 tile for 30 s. Fecal samples included human, mouse, and cat samples. Human feces were collected from five individuals using commode collectors (Fisherbrand Commode Specimen Collection System). Mouse feces were collected from two individuals and stored in 1.5 mL microcentrifuge tubes. Cat feces were collected from two individuals and stored in plastic zip-top bags. Human urine samples included samples from three female- and three male individuals, and were collected and stored in 50 mL centrifuge tubes. Soil samples included both tree rhizosphere- and bare soil. For each type, soil was collected from two adjacent sites at the Scripps Coastal Reserve down to a depth of 20 cm using a sterile trowel, and stored in plastic zip-top bags. Water samples included both fresh- and seawater, collected from two sites at the San Diego River, and two sites at Scripps Institute of Oceanography, respectively. Water was collected and stored in 50 mL centrifuge tubes. Fermented food samples included yogurt and kimchi samples. Two varieties of one brand of each food were purchased commercially and stored in 50 mL centrifuge tubes. Tissue samples included jejunum tissue from eight mice individuals: roughly 3.8 cm of the middle small intestine was removed, and any fecal matter inside was squeezed out lengthwise; each tissue section was added to a 2 mL microcentrifuge tube containing 1 mL sterile 1X PBS and roughly 40 mg sterile 1 mm silicone beads, and homogenized at 6,000 rpm for 1 min with a MagNA Lyser (Roche Diagnostics, Santa Clara, CA). The liquid homogenate from three intestinal sections from cohoused mice was pooled to create a single sample (one sample per cage). All samples were stored at –80°C within 3 h of collection. To compare limits of detection [29], we included serial dilutions of a mock community containing both bacterial and fungal taxa (*i.e.*, Zymo Research ZymoBIOMICS Mock Community Standard I, Cat#: D6300). Input cell densities ranged from 140.00-1.40E+09 cells for bacteria, and 2.66-2.66E+07 cells for fungi. Finally, to compare well-to-well contamination [32], we included plasmid-borne, synthetic 16S rRNA gene spike-ins [34] (*i.e.*, 4 ng of unique spike-in to one well of columns 1-11 in each plate), and at least five extraction blanks per plate.

DNA extraction. We compared our standardized extraction protocol that uses a 96-sample, magnetic bead cleanup format, the Qiagen MagAttract PowerSoil DNA Isolation Kit (Cat#: 27000-4-KF; Qiagen, Carlsbad, CA), against five other extraction kits: the Qiagen MagAttract PowerSoil Pro DNA Isolation Kit (Cat#: 47109; Qiagen, Carlsbad, CA), the Norgen Stool DNA Isolation Kit (Cat# 65600; Norgen Biotek, Ontario, Canada), the Applied Biosystems MagMAX Microbiome Ultra Nucleic Acid Isolation Kit (Cat#: A42357; Applied Biosystems, Foster City, CA), the Macherey-Nagel NucleoMag Food kit (Cat# 744945.1, Macherey-Nagel, Düren, Germany), and the ZymoBIOMICS 96 MagBead DNA Kit (Cat# D4302, Zymo Research, Irvine, CA). We previously showed that the MagMAX Microbiome kit performs comparably-or-better than our standardized protocol, considering a majority of the criteria included in this benchmark [33]. However, that experiment was focused on establishing the MagMAX kit as an alternative that also allows for downstream RNA-based applications, and did not examine Fungi [33].

Importantly, whereas the PowerSoil, PowerSoil Pro, Norgen, and MagMAX extraction kits employ a 96-deepwell plate format for sample lysis, the NucleoMag Food and Zymo MagBead extraction kits employ a lysis rack, which instead has 12 eight-tube strips arranged in a 96-well rack. This latter format can potentially reduce well-to-well contamination, which is known to occur primarily during the lysis step [32].

For logistical purposes, extractions were performed in two iterations (hereafter referred to as 'Round 1' and 'Round 2'), with a fresh set of samples collected in each instance. Both Round 1 and Round 2 included our standardized protocol as a baseline for comparison. Round 1 centered on the Powersoil Pro and the Norgen kits, and Round 2 the MagMAX, NucleoMag Food, and Zymo MagBead kits. For extraction, aliquots of each sample were transferred to unique wells of a 96-deepwell extraction plate (or lysis rack). For samples collected with swabs, the entire swab head was broken off into the well (or tube). For liquid samples, we transferred 200 µL. For bulk samples, we used cotton swabs to collect roughly 100 mg of homogenized material and broke the entire swab head off into the well (or tube). For each extraction protocol, all samples, including mock community dilutions, were plated in triplicate. Extractions were performed following the manufacturer's instructions. Lysis was performed with a TissueLyser II (Qiagen, Carlsbad, CA). Bead clean-ups were performed with the KingFisher Flex Purification System (ThermoFisher Scientific, Waltham, MA). Extracted nucleic acids were stored at –80°C prior to quantification of DNA yield and downstream sequencing.

16S rRNA gene, fungal ITS, and shotgun metagenomics sequencing and data analysis. We prepared DNA for 16S rRNA gene amplicon (16S), fungal ITS gene amplicon (ITS), and shallow shotgun metagenomics sequencing as described previously [10,33,35-38]. Extracts from Round 1 and Round 2 were sequenced separately on distinct runs. For bacterial/archaeal 16S data, raw sequence files were demultiplexed using Qiita [39], sub-operational taxonomic units (sOTUs) generated using Deblur with the default positive filter for 16S data [40], taxonomy assigned using QIIME2's *feature-classifier* plugin's *classify-sklearn* method with the pre-fitted classifier trained on GreenGenes V4 (13_8) data [41-44], and phylogeny inferred using QIIME2's *fragment-insertion* plugin's *sepp* method with the GreenGenes (13_8) SEPP reference [45-47]. For fungal ITS data, raw sequence files were demultiplexed using Qiita [39], sub-operational taxonomic units (sOTUs) generated using Deblur with a positive filter representing the UNITE8 reference database (dynamic OTUs, including global 97% singletons) [48], and taxonomy assigned using QIIME2's *feature-classifier* plugin's *classify-sklearn* method with a classifier trained on the UNITE8 reference database (described above) [41,48]. For shallow shotgun metagenomics data, raw sequence files were demultiplexed using BaseSpace (Illumina, La Jolla, CA), and uploaded to Qiita [39] for additional pre-processing. Demultiplexed sequence data were quality-filtered using fastp [49] and human read depleted by alignment to human reference genome GRCh38 using minimap2 [50]. Filtered reads were aligned to the Web of Life database [51] using bowtie2 [52], and alignment profiles translated to feature-tables using Woltka [53]. Raw sequence data were deposited at the European Nucleotide Archive (accession#: ERP124610) and raw and processed data are available via Qiita (Study ID: 12201). For all three datasets, subsequent normalization of sampling effort and estimation of alpha- and beta-diversity were performed using QIIME2 [9]. Analyses of taxonomic composition and beta-diversity were performed using custom Python scripts. Correlation tests and Kruskal-Wallis tests were performed in R [54]. All processing and analysis code is available on GitHub (github.com/justinshaffer/Extraction_kit_testing).

Results & Discussion.

For each of the five candidate extraction kits tested, we observed similar DNA extraction efficiency to our standardized protocol (hereafter referred to as 'PowerSoil'), with the exception of the Norgen kit, which had lower yields across all sample types except human milk (Figure 1, Figure S1A). Across the majority of sample types, the PowerSoil Pro, NucleoMag Food, MagMAX Microbiome, and Zymo MagBead kits performed comparably-or-better than PowerSoil (Figure 1, Figure S1A). We also observed similar trends in the number of quality-filtered reads generated from sequencing for each of the five candidate extraction kits as compared to PowerSoil, for 16S, fungal ITS, and shotgun metagenomics data (Figure 2, Figure S1B, Figure S2). Exceptions include the Zymo MagBead kit, which generated fewer high-quality 16S reads across samples from the built environment, water, human urine, and human skin (Figure 2E, Figure S1B), as well as the Norgen kit, which generated fewer high-quality fungal ITS reads across samples from the built environment, food, water, and soil (Figure 2G, Figure S2A). Interestingly, the reduced performance of the Norgen kit in extracting DNA (Figure 1B) did not influence its ability to generate high-quality shotgun metagenomics reads, in-line with PowerSoil (Figure 2L, Figure S2B).

Considering the limit of detection (LOD) of microbial cells, we observed differences in the ability to detect bacteria vs. fungi across the five candidate extraction kits as compared to PowerSoil (Table 1). Compared to PowerSoil, the LOD for bacteria was one order of magnitude lower for the PowerSoil Pro kit, the same for the Zymo MagBead kit, and one order of magnitude higher for MagMAX Microbiome kit (Table 1). However, when considering sample retention following filtering based on LOD thresholds – an important consideration due to the costs of obtaining/processing samples, and for maintaining reasonable sample sizes for analysis – only the PowerSoil Pro and MagMAX Microbiome kits retain ≥80% of samples, similar to PowerSoil (Table 1). The LOD for bacteria for the Norgen and NucleoMag Food kits were much higher, implying that they may not be optimal for profiling of rare taxa (Table 1). The LOD and frequency of sample retention following filtering, for fungi, was similar for all kits as compared to PowerSoil, except for the PowerSoil Pro kit, which had an LOD that was one order of magnitude higher, and also retained only 80% of samples as compared to 100% across all other protocols (Table 1). Surprisingly, the frequency of well-to-well contamination was similar among protocols (Figure 3). This is especially informative considering the unique lysis rack provided by both the NucleoMag Food and Zymo MagBead kits (see Materials & Methods), which we expected to greatly reduce the frequency of well-to-well contamination as compared to lysis in a traditional 96-deepwell plate. We suspect that well-to-well contamination can still occur when using a lysis rack in part due to movement of aerosols during uncapping tubes. We emphasize that without a reduction in well-to-well contamination provided by the lysis rack vs. a traditional plate, the roughly 20-fold increase in processing time to open 96 tubes vs. to unseal a plate (*i.e.*, ~100 s vs. 5 s, respectively) argues against adoption of the lysis rack (Figure 3). Future experiments should consider single-tube lysis, which is available for the MagMAX kit (Cat#: A42351), and has been shown to reduce well-to-well contamination [32] although at the cost of increased processing time. Similarly, automated opening/closing of individual, racked tubes, such as that offered by the Matrix Barcoded Storage Tube system (Thermo Scientific, Waltham, MA), should reduce processing time and potential aerosol transfer.

Considering the taxonomic composition of microbial communities across samples, we observed a greater degree of taxon bias among extraction kits as compared to PowerSoil for fungal taxa (*i.e.*, ITS data) as compared to bacterial/archaeal taxa (*i.e.*, 16S and shotgun metagenomics data) (Figure 4C, Figure 4D). Both the PowerSoil Pro and MagMAX Microbiome kits recovered the greatest number of exclusive fungal genera (*i.e.*, those not recovered by other protocols), with each taxon set representing roughly 19% of all fungal genera recovered in a given round of extractions (Figure 4C, Figure 4D). Similarly, both the PowerSoil Pro and MagMAX Microbiome kits shared a greater number of exclusive fungal genera with PowerSoil, as compared to the other candidate extraction kits (Figure 4C, Figure 4D). We observed a similar trend in our 16S data, except that for both rounds of extraction PowerSoil recovered the greatest number of exclusive bacterial/archaeal genera as compared to any candidate kit (Figure 4A, Figure 4B). For our shotgun metagenomics data, all candidate extraction kits except for the Norgen kit recovered a greater number of exclusive bacterial/archaeal species than PowerSoil (Figure 4E, Figure 4F). The PowerSoil Pro and NucleoMag Food kits recovered the greatest percentage of exclusive species, with the MagMAX Microbiome and Zymo MagBead kits recovering only slightly less (Figure 4E, Figure 4F). The PowerSoil Pro kit shared the greatest percentage of exclusive species with PowerSoil (16%), whereas the NucleoMag Food and MagMAX Microbiome kits shared much less (~1%) (Figure 4F).

For non-exclusive taxa, we observed strong correlations in the relative abundance estimates from each candidate extraction kit as compared to PowerSoil (Figure 5). For 16S data, the strongest correlation was observed between PowerSoil and the MagMAX Microbiome kit (Kendall's tau = 0.67) (Figure 5C), followed by the Zymo MagBead kit (tau = 0.66) (Figure 5E), and the Norgen kit (tau = 0.64) (Figure 5B). For fungal ITS data, the strongest correlation was observed with the Zymo MagBead kit (tau = 0.58) (Figure 5J), followed by the MagMAX Microbiome kit (tau = 0.47) (Figure 4H), and the PowerSoil Pro kit (tau = 0.46) (Figure 5F). For shotgun metagenomics data, the strongest correlation was observed with the Zymo MagBead kit (tau = 0.68) (Figure 5O), followed by the NucleoMag Food kit (Kendall's tau = 0.67) (Figure 5N), and the MagMAX Microbiome kit (tau = 0.59) (Figure 5M).

We also observed strong correlations in estimates of microbial community alpha-diversity from each candidate extraction kit as compared to PowerSoil (Figure 6A-E), and note in general correlations were stronger for 16S and shotgun metagenomics data as compared to for ITS data (Figure 6F-J). Specifically, correlations between candidate kits and PowerSoil for 16S alpha-diversity (*i.e.*, Faith's Phylogenetic Diversity [PD]) were all strong (tau >0.75), except for the Norgen kit, which had the weakest correlation and also the greatest sample dropout from normalization (Figure 6B). Similarly, correlations between candidate kits and PowerSoil for fungal ITS alpha-diversity (*i.e.*, Fisher's alpha) were also strong (tau >0.60), except for the PowerSoil Pro kit, which had a relatively weak relationship (Figure 6F), and the Norgen kit, which had no relationship and also significant sample dropout (Figure 6G). Correlations between candidate kits and PowerSoil for shotgun metagenomics alpha-diversity (*i.e.*, Faith's PD) were all strong (tau >0.65), and sample dropout was minimal for all protocols (Figure 6K-O).

With respect to microbial community composition, we found variation explained by bias among extraction protocols to be negligible compared with that explained by host subject identity (*i.e.*, 1-2 orders of magnitude weaker in explaining beta-diversity) (Table 2). For 16S and shotgun metagenomics data, the variation explained by extraction protocol is one order of magnitude weaker for presence/absence metrics vs. abundance-based metrics (Table 2). This supports our analysis of variation among technical replicates from the same sample, which we

observed to be small for all extraction protocols across 16S (Figure S3), fungal ITS (Figure S4), and shotgun metagenomics data (Figure S5). We also observed strong correlations in microbial community beta-diversity (*i.e.*, sample-sample distances) from each candidate extraction kit as compared to PowerSoil, and note that as for alpha-diversity, in general correlations were stronger for 16S and shotgun metagenomics data as compared to ITS data (Table S1, Table S2, Table S3). Specifically, correlations in sample-sample distances between each of the five candidate kits and PowerSoil for 16S data were strong (rho >0.75), except for in low-biomass samples processed with the Norgen kit, which exhibited no relationship with PowerSoil for two-of-four distance metrics examined (Table S1). For ITS data, correlations in sample-sample distances were consistently weaker for low biomass samples vs. high biomass samples, for all candidate extraction kits and distance metrics examined. The PowerSoil Pro kit alone had correlation coefficients >0.50 for low biomass samples and >0.75 for high biomass samples (Table S2). For shotgun metagenomics data, whereas correlations in sample-sample distances were also consistently weaker for low biomass samples vs. high biomass samples, the magnitude of the difference was smaller as compared to ITS data, and correlations for high biomass samples were strong (rho >0.85) for all candidate extraction kits and distance metrics examined (Table S3).

Importantly, whereas agreement with PowerSoil regarding the results of analyzing 16S or shotgun metagenomics data is desirable, deviation from PowerSoil among the five candidate extraction kits based on fungal ITS data was expected. In that regard, the MagMAX Microbiome kit alone consistently maintains a high degree of correlation with PowerSoil for both 16S and shotgun metagenomics data (Figure 2C, Figure 2M, Figure 5C, Figure 5M, Figure 6C, Figure 6M), while also maintaining a relatively high number of samples from both high- and low biomass subsets following normalization, across all three data layers (Table S1, Table S2, Table S3). The NucleoMag Food and Zymo MagBead kits have slightly stronger correlations with PowerSoil as compared to MagMAX for shotgun metagenomics data for certain analyses of microbial community diversity (Figure 6M-O, Table S1, Table S3). However, the MagMAX Microbiome kit recovered the greatest number of exclusive fungal genera while also sharing the greatest number of exclusive fungal genera with PowerSoil (Figure 4D). Although the PowerSoil Pro kit also recovered a similar frequency of exclusive fungal genera (Figure 4C), the increased sample dropout following normalization for that kit vs. the MagMAX Microbiome kit (*i.e.*, particularly for low biomass samples) (Table S1, Table S2, Table S3), increased processing time (*i.e.*, approximately 3.5 h for PowerSoil and PowerSoil Pro vs. 1.0 h for MagMAX Microbiome), as well as the increased cost of consumables (*i.e.*, 3.5X reagent reservoirs and 7X tips for PowerSoil and PowerSoil Pro vs. MagMAX Microbiome) combined with previous work showing that the MagMAX kit can also extract high-quality RNA from similar samples [33], argue strongly for the use of the MagMAX Microbiome kit. However, the PowerSoil Pro kit is a good alternative if there are no downstream RNA applications, and if time and cost are not important factors.

Conclusions.

We conclude that the MagMAX Microbiome extraction kit is comparable to our standardized PowerSoil protocol with respect to characterizing microbial community composition using both 16S and shotgun metagenomic data, and is optimal compared to other candidate kits and our standardized protocol for doing so using fungal ITS data, as it recovers the greatest number of unique fungal genera. The PowerSoil Pro kit is a good alternative, as it excels in the same

regards, but it does not extract RNA and is a more time- and cost-intensive protocol, as compared to the MagMAX Microbiome kit. Regardless, data from the PowerSoil, PowerSoil Pro, and MagMAX Microbiome extraction kits should allow for comparisons such as meta-analysis across 16S, ITS, and shotgun metagenomics data produced using those protocols and downstream processing and analytical methods similar to those used here. In addition to recovering a greater number of fungal taxa, the more rapid processing time, and use of fewer consumables highlight the MagMAX Microbiome kit as a comparable and efficient alternative to the PowerSoil protocol that also optimizes downstream applications, including fungi.

Future perspective.
Future efforts should continue to focus on optimizing microbiological and molecular methods that capture all organisms in a sample regardless of their evolutionary history, and from a diversity of sample types such as those examined here. Such methods provide invaluable resources and should serve as gold standards to be adopted widely by the community [56]. In parallel, further advances in computational methods should focus on reducing technical effects in meta-analyses across studies using distinct methods [6,39]. In concert, such advances will allow us to maximize our understanding of microbial communities and to harness that knowledge in part to foster human and environmental sustainability.

Author contributions.
JP Shaffer, CS Carpenter, RA Salido, JJ Minich, G Humphrey, AD Swafford, and R Knight designed the study; JP Shaffer, CS Carpenter, RA Salido, M Bryant, and G Humphrey provided samples; JP Shaffer, CS Carpenter, and T Schwartz performed extractions; RA Salido, M Bryant, K Sanders, and G Humphrey performed quality control and sequencing; JP Shaffer, C Martino, and RA Salido performed data analyses; JP Shaffer wrote the manuscript, with contributions from all authors.

Acknowledgements.
We thank S Miller-Montgomery for helping to conceptualize the study; C Marotz, P Belda-Ferre, L Bode, C Brennan, M Estaki, T Kosciolek, SJ Song, J Toronczak, and L Zaramela for providing samples; the Scripps Coastal Reserve for permitting collection of soil samples; L Zaramela for providing synthetic plasmids for well-to-well contamination assay; J DeReus for assistance with data processing; G Ackermann for curating metadata and making the data publicly available; and SJ Song and KJ Cavagnero for assistance with visualizing taxon abundance correlations.

Financial disclosures.
JP Shaffer was supported by NIH San Diego Institutional Research and Academic Career Development Award (5K12GM068524-17) and the United States Department of Agriculture - National Institute of Food and Agriculture (USDA-NIFA) (2019-67013-29137). C Martino was supported by NIH (1RF1-AG058942-01) and Semiconductor Research Corporation and Defense Advanced Research Projects Agency (SRC/DARPA) (GI18518). JJ Minich was supported by NSF (2011004). G Humphrey was supported by NIH (U19AG063744,U01 AI124316), Office of

Naval Research (ONR) (N00014-15-1-2809) and the Emerald Foundation (3022). R Knight was supported by NIH (1RF1-AG058942-01, 1DP1AT010885, R01HL140976, R01DK102932, R01HL134887), USDA-NIFA (2019-67013-29137), SRC/DARPA(GI18518), CCFA (675191), ONR (N00014-15-1-2809) and the Emerald Foundation (3022).

Ethical conduct of research.
The human subjects work conducted here is approved through UCSD IRB#150275.

Executive summary.
1. We compared our previously established, standardized protocol for DNA extraction against five alternative DNA extraction kits.
2. We included a diverse panel of sample types ranging from host-associated to environmental.
3. We also included controls for detecting well-to-well contamination and the limit of detection of microbial cells.
4. We observed sample type-specific differences in DNA extraction efficiency among all extraction protocols.
5. Sample type and host identity were stronger drivers of microbial community beta-diversity as compared to the extraction protocol used.
6. We identify one protocol that generates high-quality fungal ITS data, and produces 16S- and shotgun metagenomics data with high similarity to our established protocol with respect to microbial community alpha-diversity, beta-diversity, and taxonomic composition.
7. The similarity between the optimal protocol and our existing one will allow for meta-analyses across both with negligible technical bias.

References.
1. Kelly CR, Ihunnah C, Fischer M, *et al.* Fecal microbiota transplant for treatment of *Clostridium difficile* infection in immunocompromised patients. *Am. J. Gastroenterol.* 109(7), 1065-1071 (2014).
2. Panke-Buisse K, Poole AC, Goodrich JK, Ley RE, Kao-Kniffin J. Selection on soil microbiomes reveals reproducible impacts on plant function. *ISME J.* 9, 980-989 (2015).
3. Bell TH, Stefani FOP, Abram K, *et al.* A diverse soil microbiome degrades more crude oil than specialized bacterial assemblages obtained in culture. *Appl. Environ. Microbiol.* 82(18), 5530-5541 (2016).
4. Mills, RH, Dulai PS, Vásquez-Baeza Y, *et al.* Multi-omics analysis of the ulcerative colitis gut microbiome links *Bacteroides vulgatus* proteases with disease severity. *Nat. Microbiol*. 7, 262-276 (2022).
5. Dominguez-Bello MG, Godoy-Vitorino F, Knight R, and Blaser MJ. Role of the microbiome in human development. *Gut* 68, 1108-1114 (2019).
6. Poore GD, Kopylova E, Zhu Q, *et al.* Microbiome analysis of blood and tissues suggest cancer diagnostic approach. *Nature* 579, 567-574 (2020).
7. Erdman, S. Oxytocin and the microbiome. *Curr. Opin. Endocrin. Metabol. Res.* 19, 8-14 (2021).

8. Knight R, Vrbanac A, Taylor BC, *et al.* Best practices for analysing microbiomes. *Nat. Rev. Microbiol.* 16, 410-422 (2018).
9. Bolyen E, Rideout JR, Dillon MR, *et al.* Reproducible, interactive, scalable, and extensible microbiome data science using QIIME2. *Nat. Biotechnol.* 37, 852-857 (2019).
10. Sanders JG, Nurk S, Salido RA, *et al.* Optimizing sequencing protocols for leaderboard metagenomics by combining long and short reads. *Genome Biol.* 20, 1-14.226 (2019).
11. Parada AE, Needham DM, Fuhrman JA. Every base matters: assessing small subunit rRNA primers for marine microbiomes with mock communities, time series and global field samples. *Environ. Microbiol.* 18(5), 1403-1414 (2016).
12. Bjerre RD, Hugerth LW, Boulund F, Seifert FM, Johansen JD, Engstrand L. Effects of sampling strategy and DNA extraction on human skin microbiome investigations. *Sci. Rep.* 9, 1-11.17287 (2019).

*Important for understand the influence of technical factors on analysis of microbial communities

13. Marotz C, Cavagnero KJ, Song SJ, *et al.* Evaluation of the effect of storage methods on fecal, saliva, and skin microbiome composition. *mSystems* 6(2), e01329-20 (2021).

**Highlights the importance of considering how samples are maintained prior to processing for analysis of microbial communities

14. Thompson LR, Sanders JS, McDonald D, *et al.* A communal catalogue reveals Earth's multiscale microbial diversity. *Nature* 551, 457-463 (2017).
15. Lloyd-Price J, Arze C, Ananthakrishnan AN, *et al.* Multi-omics of the gut microbial ecosystem in inflammatory bowel disease. *Nature* 569, 655-662 (2019).
16. Nayfach S, Roux S, Seshadri R, *et al.* A genomic catalog of Earth's microbiomes. *Nat. Biotechnol.* 39, 499-509 (2020).
17. Dean R, Van Kan JAL, Pretorius ZA, *et al.* The top 10 fungal pathogens in molecular plant pathology. *Mol. Plant Pathol.* 13(4), 414-430 (2012).
18. Bebber DP and Gurr SJ. Crop-destroying fungal and oomycete pathogens challenge food security. *Fungal Genet. Biol.* 74, 62-64 (2015).
19. Seyedmousavi S, Bosco SMG, Hoog S, *et al.* Fungal infections in animals: a patchwork of different situations. *Medical Mycology* 56, S165-S187 (2018).
20. Scheele BC, Pasmans F, Skerratt LF, *et al.* Amphibian fungal panzootic causes catastrophic and ongoing loss of biodiversity 363(6434), 1459-1463 (2019).
21. Cheng TL, Reichard JD, Coleman JTH, *et al.* The scope and severity of white-nose syndrome on hibernating bats in North America. *Conserv. Biol.* 35(5), 1586-1597 (2021).
22. Ma Z, Guo D, Xu X, *et al.* Evolutionary history resolves global organization of root functional traits. *Nature* 555, 94-97 (2018).
23. Simard SW. Mycorrhizal networks facilitate tree communication, learning, and memory. In: Baluska F, Gagliano M, Witzany G (eds) Memory and Learning in Plants. Signaling and Communication in Plants. Springer, Cham. (2018). doi: 10.1007/978-3-319-75596-0_10
24. Tedersoo L, Bahram M, and Zobel M. How mycorrhizal associations drive plant population and community biology. *Science* 367(6480), 867 (2020).
25. Aykut B, Pushalkar S, Chen R, *et al.* The fungal mycobiome promotes pancreatic oncogenesis via activation of MBL. *Nature* 574, 264-267 (2019).
26. Coker OO, Nakatsu G, Dai RZ, *et al.* Enteric fungal microbiota dysbiosis and ecological alterations in colorectal cancer. *Gut* 68, 654-662 (2019).

27. Liu NN, Jiao N, Tan JC, *et al.* Multi-kingdom microbiota analysis identify bacterial-fungal interactions and biomarkers of colorectal cancer across cohorts. *Nat. Microbiol.* 7, 238-250 (2022).
28. Marotz C, Amir A, Humphrey G, Gaffney J, Gogul G, Knight R. DNA extraction for streamlined metagenomics of diverse environmental samples. *BioTechniques* 62(6), 290-293. (2017).

**Important for understanding differences in DNA extraction methods, particularly different bead clean-up methods, for downstream analysis of microbial communities

29. Minich JJ, Zhu Q, Janssen S, Hendrickson SR, *et al.* KatharoSeq Enables High-Throughput Microbiome Analysis from Low-Biomass Samples. *mSystems* 3(3), 1-16.e00218.17 (2018).

**Important for understanding differences in DNA extraction methods for regular or high- vs. low-biomass sample types for analysis of microbial communities

30. Salter SJ, Cox MJ, Turek EM, *et al.* Reagent and laboratory contamination can critically impact sequence-based microbiome analysis. *BMC Biol.* 12, 1-12.87 (2014).
31. Eisenhofer R, Minich JJ, Marotz C, Cooper A, Knight R, Weyrich LS. Contamination in low microbial biomass microbiome studies: issues and recommendations. *Trends Microbiol.* 27(2), 105-117 (2019).
32. Minich JJ, Sanders JG, Amir A, Humphrey G, Gilbert JA, Knight R. Quantifying and understanding well-to-well contamination in microbiome research. *mSystems* 4(4), 1-8.e00186-19 (2019).
33. Shaffer JP, Marotz C, Belda-Ferre P, *et al.* A comparison of DNA/RNA extraction protocols for high-throughput sequencing of microbial communities. *Biotechniques* 70, 149-159 (2021).
34. Tourlousse DM, Yoshiike S, Ohashi A, Matsukura S, Noda N, Sekiguchi Y. Synthetic spike-in standards for high-throughput 16S rRNA gene amplicon sequencing. *Nucleic Acids Res.* 45(4), 1-14.e23 (2016).
35. Caporaso JG, Lauber CL, Walters WA, *et al.* Ultra-high-throughput microbial community analysis on the Illumina HiSeq and MiSeq platforms. *ISME J.* 6, 1621-1624 (2012).
36. Minich JJ, Humphrey G, Benitez RAS, *et al.* High-throughput miniaturized 16S rRNA amplicon library preparation reduces costs while preserving microbiome integrity. *mSystems* 3(6), 1-8.e00166-18 (2018).
37. Hillmann B, Al-Ghalith GA, Shields-Cutler RR, *et al.* Evaluating the information content of shallow shotgun metagenomics. *mSystems* 3(6), 1-12.e00069-18 (2018).
38. Shaffer JP, Nothias LF, Thompson LR, *et al.* Multi-omics profiling of Earth's biomes reveals that microbial and metabolite composition are shaped by the environment. *bioRxiv* (2022) doi: 10.1101/2021.06.04.446988
39. Gonzalez A, Navas-Molina JA, Kosciolek T, *et al.* Qiita: rapid, web-enabled microbiome meta-analysis. *Nat. Methods* 15, 796-798 (2018).
40. Amir A, McDonald D, Navas-Molina JA, *et al.* Deblur rapidly resolves single-nucleotide community sequence patterns. *mSystems* 2(2), 1-7.e00191-16 (2017)
41. Pedregosa F, Varoquaux G, Gramfort A, *et al.* Scikit-learn: machine learning in python. *J. Machine Learn. Res.* 12, 2825-2830 (2011)
42. Robeson MS, O'Rourke DR, Kaehler BD, *et al.* RESCRIPt: Reproducible sequence taxonomy reference database management for the masses. *bioRxiv* (2020). doi: 10.1101/2020.10.05.326504

43. Bokulich NA, Kaehler BD, Rideout JR, *et al.* Optimizing taxonomic classification of marker-gene amplicon sequences with QIIME2's q2-feature-classifier plugin. *Microbiome* 6, 90 (2018)
44. McDonald D, Price MN, Goodrich J, *et al.* An improved Greengenes taxonomy with explicit ranks for ecological and evolutionary analysis of bacteria and archaea. *ISME J.* 6, 610-618 (2012)
45. Eddy SR. Accelerated profile hmm searches. *PLOS Computation. Biol.* 7(10), 1-16 (2011)
46. Janssen S, McDonald D, Gonzalez A, *et al.* Phylogenetic placement of exact amplicon sequences improves associations with clinical information. *mSystems* 3(3), e00021-18 (2018)
47. Matsen FA, Kodner RB, and Armbrust EV. Pplacer: linear time maximum likelihood and Bayesian phylogenetic placement of sequences onto a fixed reference tree. *BMC Bioinformat.* 11(1), 538 (2010)
48. Abarenkov K, Zirk A, Piirmann T, *et al.* UNITE QIIME relese for Fungi. Version 10.05.2021. *UNITE Community* (2021) doi: 10.15156/BIO/1264708
49. Shifu C, Yanqing Z, Chen Y, *et al.* fastp: an ultra-fast all-in-one FASTQ preprocessor. *Bioinformat.* 34(17), i884-i890 (2018)
50. Li H. Minimap2: pairwise alignment for nucleotide sequences. *Bioinformat.* 34(18), 3094-3100 (2018)
51. Zhu Q, Mai U, Pfeiffer W, *et al.* Phylogenomics of 10,575 genomes reveals evolutionary proximity between domains Bacteria and Archaea. *Nat. Commun.* 10, 1-14.5477 (2019).
52. Langmead B, Salzberg SL. Fast gapped-read alignment with Bowtie 2. *Nat. Methods* 9(4), 357-359 (2012).
53. Zhu Q, Huang S, Gonzalez A, *et al.* OGUs enable effective, phylogeny-aware analysis of even shallow metagenome community structures. *bioRxiv* (2021) doi: 10.1101/2021.04.04.438427
54. R Core Team. R: A language and environment for statistical computing. R Foundation for Statistical Computing, Vienna, Austria. (2022) https://www.R-project.org/
55. Greathouse KL, Sinha R, Vogtmann E. DNA extraction for human microbiome studies: the issue of standardization. *Genome Biol.* 20, 2-4.212 (2019).

Tables and Figures

Table 1. Limits of detection (LOD) of microbial cells across extraction kits. Titrations of a mock community containing known numbers of cells of bacterial and fungal species (see Materials & Methods) was used to identify the number of reads needed per sample, to meet various thresholds of detection (*i.e.*, the percentage of reads mapped to expected taxa vs. background contaminants). Read depths corresponding to a threshold of 50% were used for filtering samples prior to community analyses of bacterial/archaeal 16S- and fungal ITS data, as recommended [29]. The retention of samples following filtering based on the read depth for each threshold, as well as LOD estimates for bacterial and fungal cells are shown for 16S- and ITS data, respectively. Round 1 and Round 2 indicate different sequencing runs, and because sampling effort was not normalized here such to compare absolute read counts, comparisons should not be made across sequencing runs.

			16S				ITS			
Round	Extraction kit	Threshold (%)	LOD	Read depth	Samples retained	Samples retained (%)	LOD	Read depth	Samples retained	Samples retained (%)
1	PowerSoil	50	1.40E+03	73	81	86	2.66E+00	3	94	100
		80	1.40E+05	449	55	59	2.66E+02	223	45	48
		90	1.40E+05	1812	43	46	> 2.66E+07	199,755	0	0
		95	1.40E+08	8676	39	41	> 2.66E+07	165,759,100,584	0	0
	PowerSoil Pro	50	1.40E+02	46	79	84	2.66E+01	49	70	80
		80	1.40E+02	692	61	65	2.66E+04	1,094	39	45
		90	1.40E+06	7520	33	35	2.66E+05	18,669	14	16
		95	> 1.40E+09	145206	0	0	> 2.66E+07	698,158	0	0
	Norgen Stool	50	1.40E+07	1960	18	19	2.66E+00	2	88	100
		80	1.40E+07	4705	12	13	2.66E+05	850	7	8
		90	1.40E+08	8224	10	10	> 2.66E+07	314,049,798	0	0
		95	1.40E+08	14215	9	10	> 2.66E+07	> 1.00E+12	0	0
2	PowerSoil	50	1.40E+02	88	93	97	2.66E+00	3	91	100
		80	1.40E+02	3224	80	83	2.66E+00	6	91	100
		90	> 1.40E+09	88894	0	0	2.66E+00	12	86	95
		95	> 1.40E+09	6228705	0	0	2.66E+00	24	75	82
	MagMAX Microbiome	50	1.40E+03	1286	79	82	2.66E+00	5	92	100
		80	1.40E+04	4147	66	69	2.66E+00	479	64	70
		90	1.40E+04	8970	63	66	> 2.66E+07	451,442	0	0
		95	1.40E+04	19454	39	41	> 2.66E+07	176,467,642,943	0	0
	NucleoMag Food	50	1.40E+05	8379	61	64	2.66E+00	1	88	100
		80	1.40E+05	14121	45	47	2.66E+00	2	88	100
		90	1.40E+06	19430	27	28	2.66E+02	74	69	78
		95	1.40E+07	26321	18	19	> 2.66E+07	26,901,301	0	0
	Zymo MagBead	50	1.40E+02	489	42	44	2.66E+00	1	90	100
		80	1.40E+02	1838	32	33	2.66E+00	4	90	100
		90	1.40E+06	4531	22	23	2.66E+01	466	38	42
		95	1.40E+06	11445	10	10	> 2.66E+07	5,179,906,841	0	0

Table 2. Results from a forward, stepwise model selection of factors influencing microbial community beta-diversity in this study. Values are based on permutation tests of variation explained by redundancy analysis (*n* = 5,000 runs), done separately for unique distance metrics for 16S, ITS, and shotgun metagenomic data. The full model included extraction round (*i.e.*, round 1 vs. 2), sample biomass (*i.e.*, high vs low biomass), sample type, host subject identity, and extraction protocol as model variables. 16S data were rarefied to 10,000 quality-filtered reads per sample or had samples with fewer than 10,000 reads excluded when using RPCA distances (*n* = 640 samples). Fungal ITS data were rarefied to 630 quality-filtered reads per sample or had samples with fewer than 630 reads excluded when using RPCA distances (*n* = 978 samples). Shotgun metagenomic data were rarefied to 2,100 host- and quality-filtered reads per sample or had samples with fewer than 2,100 reads excluded when using RPCA distances (*n* = 1,044 samples). Rarefaction depths were selected to maintain at least 75% samples (50% for fungal ITS data) from both high- and low-biomass datasets. AIC: Akaike information criterion; df: degrees of freedom; RPCA: Robust principal components analysis (*i.e.*, Robust Aitchison distance).

Data type	Distance metric	Factor	Adjusted R^2	df	AIC	F	p-value
16S	Unweighted UniFrac	Host identity	0.93	60	-979.83	152.03	0.0002
	Unweighted UniFrac	Extraction kit	0.001	6	-988.95	3.20	0.0004
	Weighted UniFrac	Host identity	0.84	60	-428.10	58.62	0.0002
	Weighted UniFrac	Extraction kit	0.02	6	-533.75	19.27	0.0002
	Jaccard	Host identity	0.96	60	-1234.51	231.05	0.0002
	Jaccard	Extraction kit	0.002	6	-1254.66	4.92	0.0002
	RPCA	Host identity	0.89	60	-644.89	86.15	0.0002
	RPCA	Extraction kit	0.004	6	-663.81	4.73	0.0002
ITS	Jaccard	Host identity	0.80	59	-191.58	33.90	0.0002
	Jaccard	Extraction kit	0.02	6	-235.28	8.51	0.0002
	RPCA	Host identity	0.72	59	-30.05	22.32	0.0002
	RPCA	Extraction kit	0.02	6	-62.07	6.64	0.0002
Metagenomic	Unweighted UniFrac	Host identity	0.92	65	-1063.58	141.03	0.0002
	Unweighted UniFrac	Extraction kit	0.005	6	-1107.59	8.79	0.0002
	Weighted UniFrac	Host identity	0.87	65	-672.15	81.26	0.0002
	Weighted UniFrac	Extraction kit	0.02	6	-807.08	24.46	0.0002
	Jaccard	Host identity	0.93	65	-1195.00	168.79	0.0002
	Jaccard	Extraction kit	0.003	6	-1225.27	6.57	0.0002
	RPCA	Host identity	0.85	65	-579.25	70.95	0.0002
	RPCA	Extraction kit	0.01	6	-633.10	10.40	0.0002

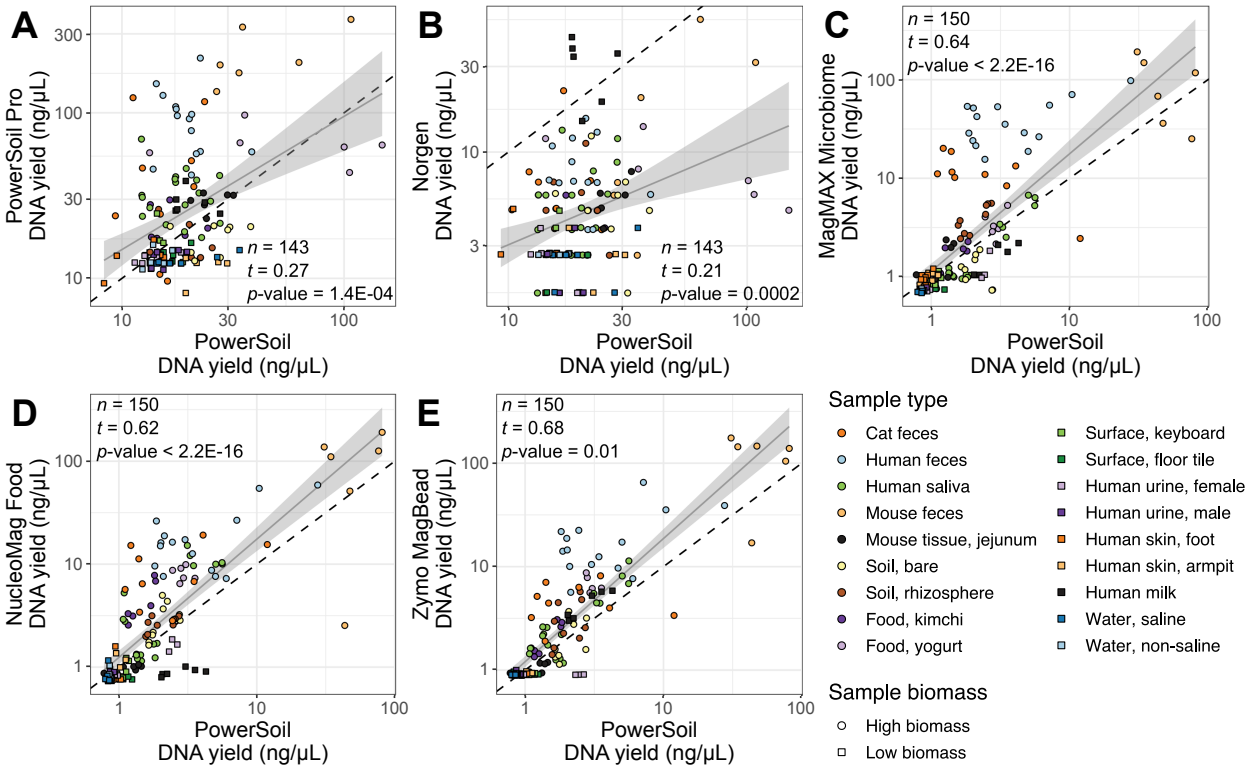

Figure 1. DNA yield (ng/µL) per sample for each candidate extraction kit (*y*-axis) as compared to our standardized protocol (*x*-axis). **(A)** PowerSoil Pro. **(B)** Norgen Stool. **(C)** MagMAX Microbiome. **(D)** NucleoMag Food. **(E)** Zymo MagBead. For all panels, colors indicate sample type and shapes sample biomass, and dotted gray lines indicate 1:1 relationships between methods. Results from tests for correlation between per-sample DNA yield for each respective candidate kit vs. from our standardized protocol, are shown (t = Kendall's tau). For significant correlations, results from a linear model including a 95% confidence interval for predictions are shown. Both axes are presented in a $\log_{10}$ scale. A miniaturized, high-throughput Quant-iT PicoGreen dsDNA assay was used for quantification, with a lower limit of 0.1 ng/µL. Yields below this value were estimated by extrapolating from a standard curve.

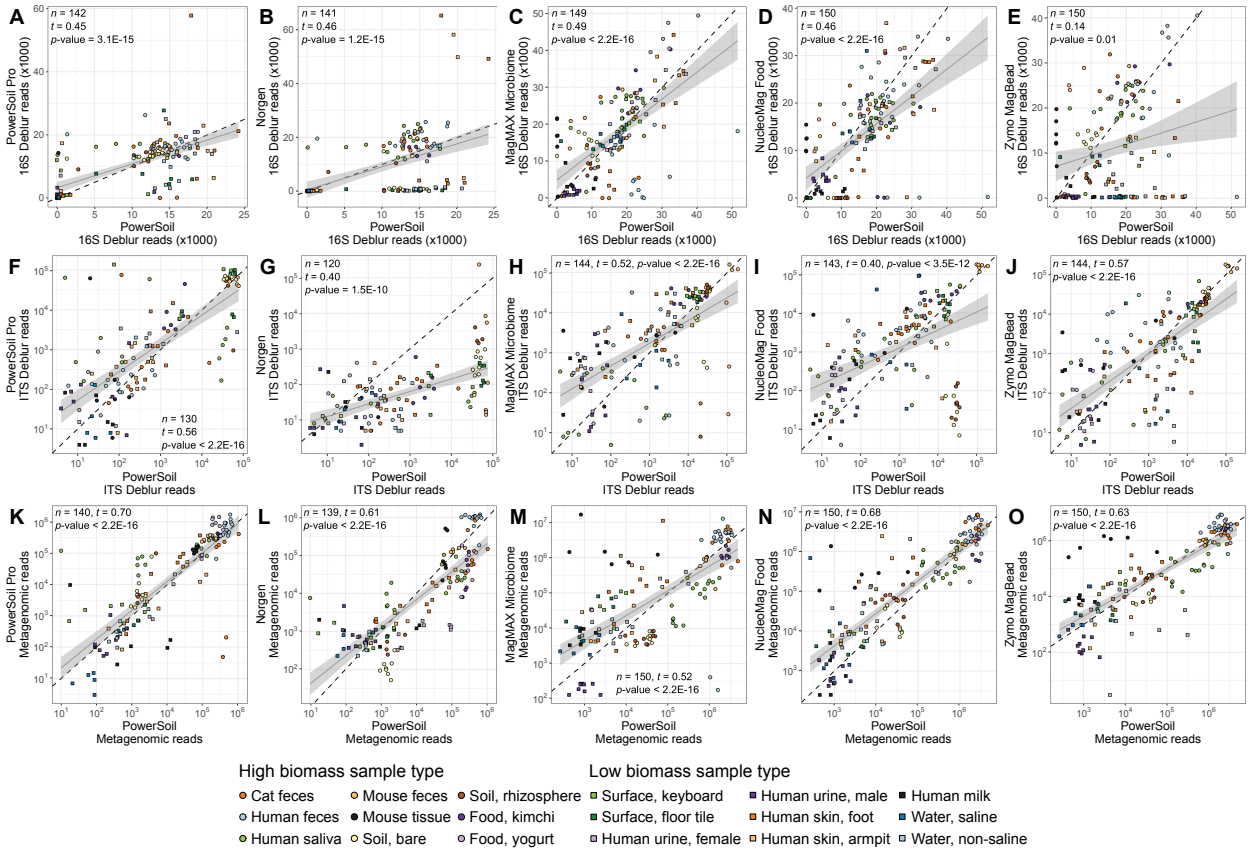

Figure 2. Sequences per sample for each candidate extraction kit (*y*-axis) as compared to our standardized protocol (*x*-axis). **(A-E)** 16S data. **(F-J)** Fungal ITS data. **(K-P)** Shotgun metagenomic data. For each panel, colors indicate sample type and shapes sample biomass, and dotted gray lines indicate a 1:1 relationship between methods. For each dataset, results from tests for correlation between read counts from each respective candidate kit vs. from our standardized protocol, are shown (t = Kendall's tau). For significant correlations, results from a linear model including a 95% confidence interval for predictions are shown. Both axes are presented in a $\log_{10}$ scale.

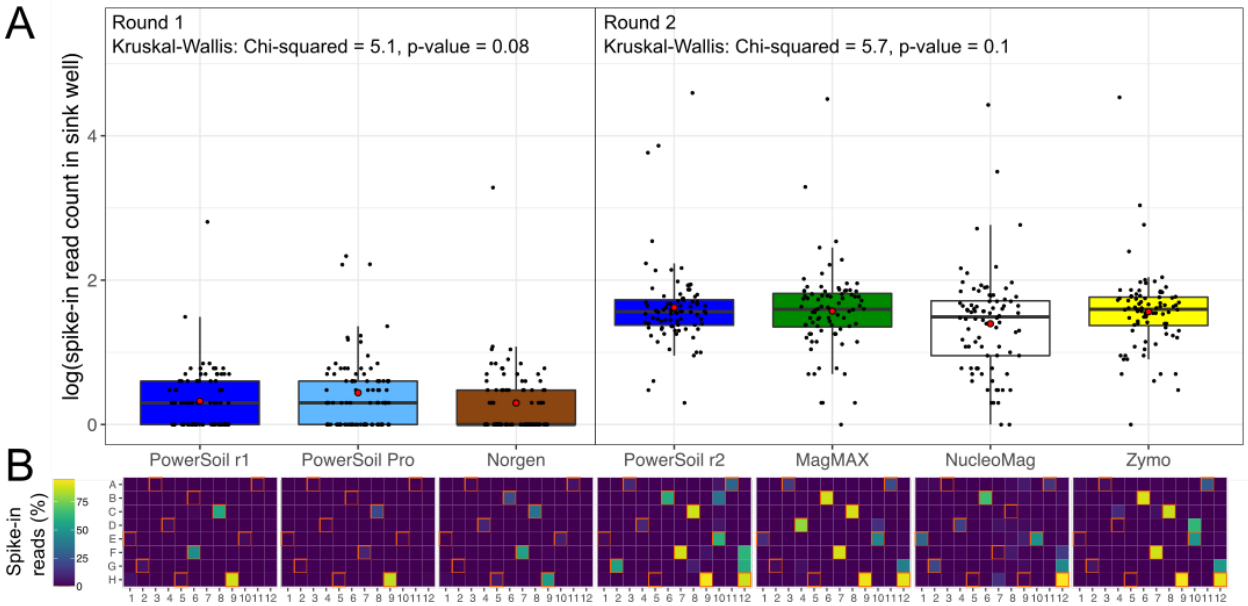

Figure 3. Well-to-well contamination across candidate extraction kits as compared to our standardized protocol. Plasmids harboring synthetic 16S sequences were spiked into a single well per plate column (*i.e.*, 1-11) of each high-biomass sample plate prior to extraction. **(A)** The number of reads matching synthetic 16S sequences was quantified for all wells that did not receive a spike-in (*i.e.*, sink wells). Round 1 and Round 2 indicate different sequencing runs, and because sampling effort was not normalized here such to compare absolute read counts, comparisons should not be made across sequencing runs. For each sequencing run, results from a Kruskal-Wallis test are shown. **(B)** The percentage of spike-in reads among all reads per well shown as a heatmap. Wells into which plasmids were spiked (*i.e.*, source wells) are outlined in orange.

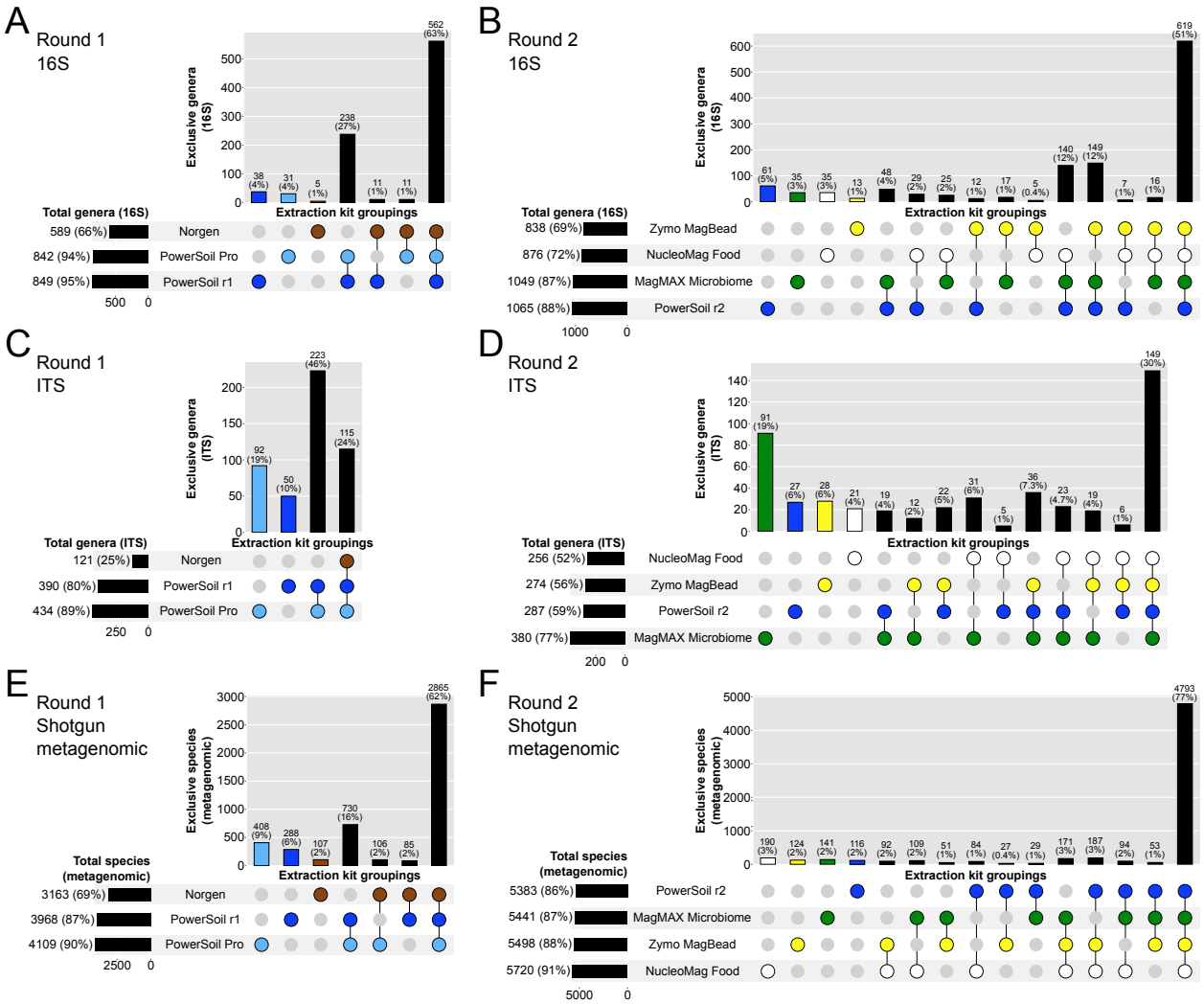

Figure 4. Taxonomic bias among extraction protocols. Upset plots showing **(A, B)** genera for bacterial/archaeal 16S data, **(C, D)** genera for fungal ITS data, and **(E, F)** species for bacterial/archaeal metagenomics data, highlighting taxa shared among extraction protocols. Values indicate counts and percentages are respective to all taxa across all protocols. Associations representing <5 taxa were excluded for clarity. Round 1 and Round 2 indicate different sequencing runs, and because sampling effort was not normalized here such to compare absolute taxon counts, comparisons of counts (*i.e.*, vs. percentages) should not be made across sequencing runs.

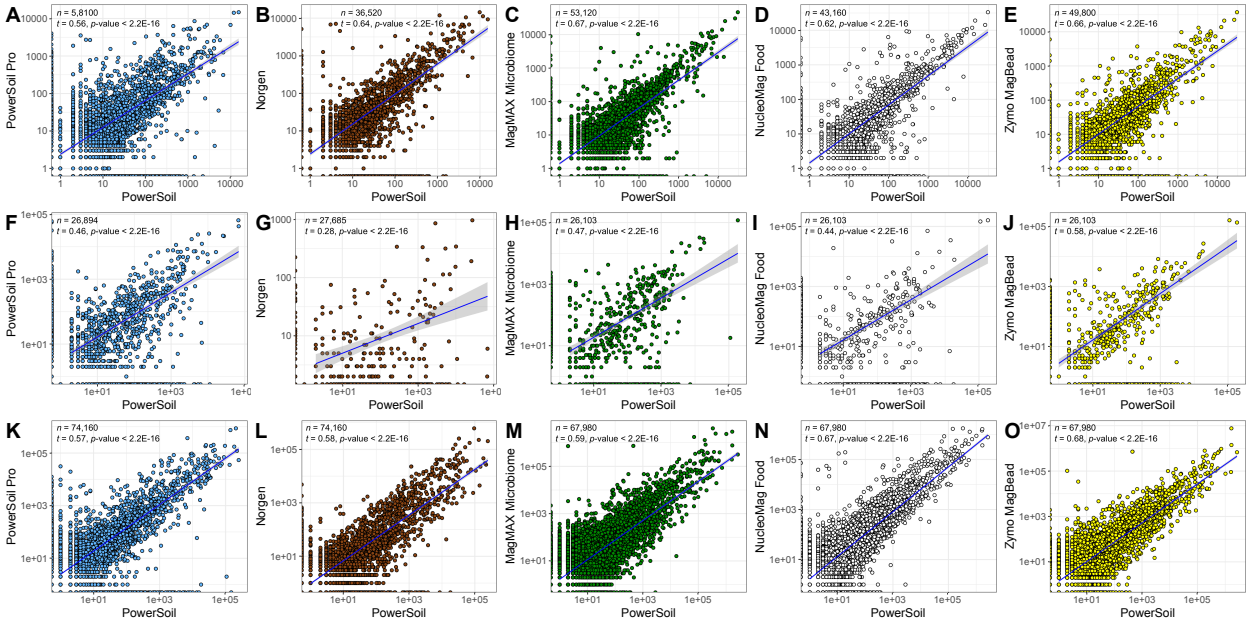

Figure 5. Taxon relative abundances across all samples for each candidate extraction kit (*y*-axis) as compared to our standardized protocol (*x*-axis). Colors indicate candidate kits. **(A-E)** 16S data, where each point represents a bacterial/archaeal genus. **(F-J)** Fungal ITS data, where each point represents a fungal genus. **(K-O)** Shotgun metagenomic data, where each point represents a bacterial/archaeal genus. For each dataset, results from tests for correlation between taxon abundances from each respective candidate kit vs. our standardized protocol, are shown (t = Kendall's tau). For significant correlations, results from a linear model including a 95% confidence interval for predictions are shown. Both axes are presented in a $\log_{10}$ scale.

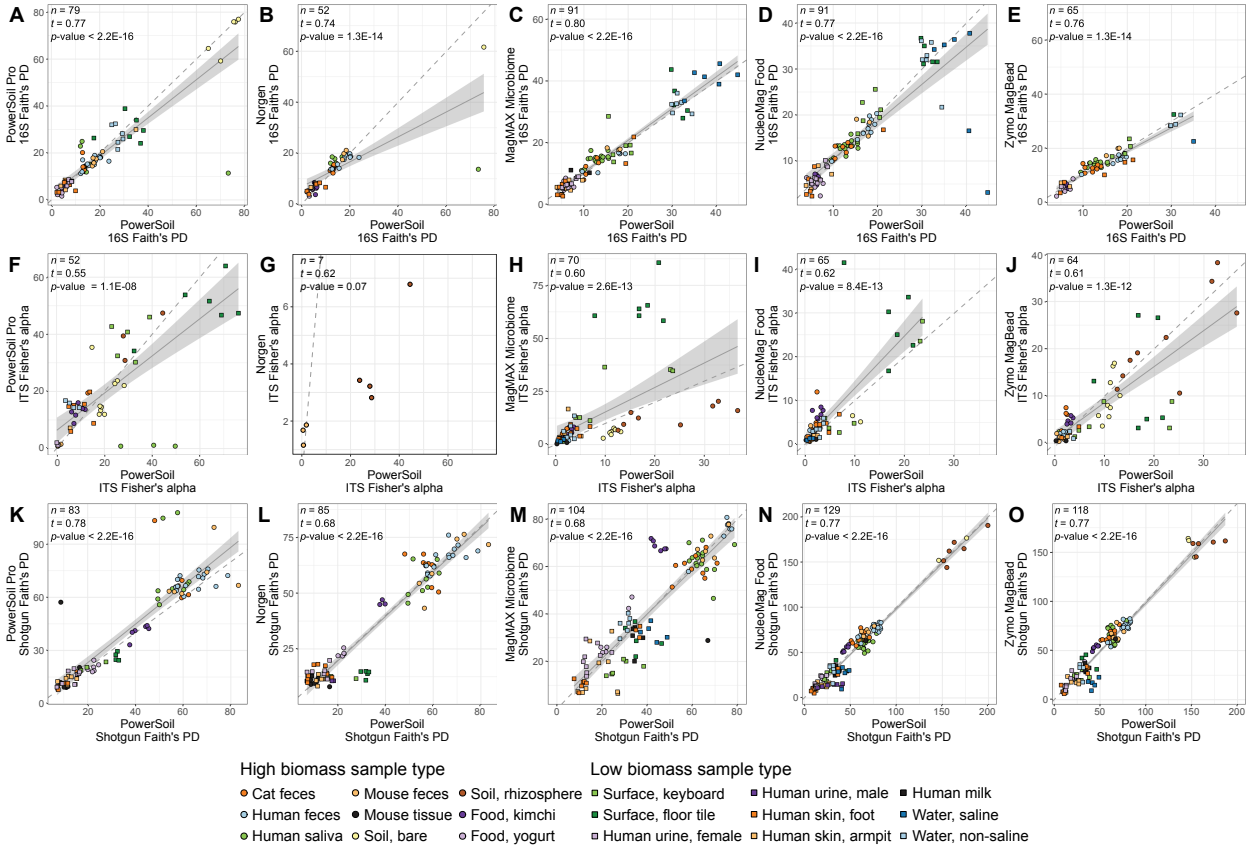

Figure 6. Alpha-diversity per sample across sample types for each candidate extraction kit (*y*-axis) as compared to our standardized protocol (*x*-axis). **(A-E)** 16S data. **(F-J)** Fungal ITS data. **(K-P)** Shotgun metagenomic data. For each panel, colors indicate sample type and shapes sample biomass, and dotted gray lines indicate a 1:1 relationship between methods. Results from tests for correlation between alpha-diversity values from each respective candidate kit vs. from our standardized protocol, are shown (t = Kendall's tau). For significant correlations, results from a linear model including a 95% confidence interval for predictions are shown. Sample types absent from any panel lacked representation by the respective candidate extraction kit and our standardized protocol.